7054–7067 *Nucleic Acids Research, 2010, Vol. 38, No. 20* *Published online 22 June 2010*
doi:10.1093/nar/gkq566

Time-dependent increase in ribosome processivity

Jennifer M. Bonderoff and Richard E. Lloyd*

Department of Molecular Virology and Microbiology and Interdepartmental Program in Cell and Molecular Biology, Baylor College of Medicine, One Baylor Plaza, Houston, TX 77030, USA

Received March 19, 2010; Revised May 17, 2010; Accepted June 4, 2010

ABSTRACT

We created a novel tripartite reporter RNA to separately and simultaneously examine ribosome translation rates at the 5′- and 3′-ends of a large open reading frame (ORF) *in vitro* in HeLa cell lysates. The construct contained *Renilla* luciferase (RLuc), β-galactosidase and firefly luciferase (FLuc) ORFs linked in frame and separated by a viral peptide sequence that causes cotranslational scission of emerging peptide chains. The length of the ORF contributed to low ribosome processivity, a low number of initiating ribosomes completing translation of the entire ORF. We observed a time-dependent increase in FLuc production rate that was dependent on a poly(A) tail and poly(A)-binding protein, but was independent of eIF4F function. Stimulation of FLuc production occurred earlier on shorter RNA templates. Cleavage of eIF4G at times after ribosome loading on templates occurred did not cause immediate cessation of 5′-RLuc translation; rather, a delay was observed that shortened when shorter templates were translated. Electron microscopic analysis of polysome structures in translation lysates revealed a time-dependent increase in ribosome packing and contact that correlated with increased processivity on the FLuc ORF. The results suggest that ORF transit combined with PABP function contribute to interactions between ribosomes that increase or sustain processivity on long ORFs.

INTRODUCTION

Protein synthesis is an energy-intensive process, and the integrity of its products are critical to the viability of the organism. Translation has long been divided into three phases: initiation, elongation and termination; however, a growing body of evidence suggests that a fourth phase, ribosome recycling, constitutes a biochemically distinct translation phase (1,2). The highly regulated initiation process is rate limiting in the majority of experimental systems and has been intensely studied (3). Considerable energy is spent on the regulation of translation initiation by myriad factors and signal transduction pathways. However, translation elongation, the most energy-intensive phase, termination and ribosome recycling are also regulated processes, but are less well understood.

Ribosome processivity, the probability that a ribosome that has initiated translation on an open reading frame (ORF) will complete elongation and terminate at the ORF's cognate stop codon, depends to some extent on the ORF and system under study. Ribosome processivity in *Escherichia coli* has been reported to decrease exponentially with increasing ORF length (4). There is debate over whether processivity decreases with increased ORF length in eukaryotes. The overall ribosome density on short ORFs is higher than that on longer ORFs in *Saccharomyces cerevisiae* (5). More recently, a ribosome density mapping procedure was used to conclude that ribosome processivity within an ORF was high but mRNAs with longer ORFs had much lower ribosome density due to lower initiation rates (6). In contrast to this view, deep sequencing of RNA fragments protected by ribosome footprints have shown that within a given ORF, ribosomes are more likely to occupy 5′-proximal codons than 3′-proximal codons (7), implying that overall processivity is lower than expected. On balance, the available data suggest that a reduced fraction of initiating ribosomes complete translation of the entire ORF, particularly on longer ORFs.

Along a different vein, ~30% of the peptides produced in mammalian cells are degraded shortly after synthesis (8,9). Some are thought to be degraded by cotranslational processes (10,11). Wheatley *et al.* (9) first theorized that these rapidly degraded peptides represented not just a select pool of proteins with rapid turnover but a sampling of all proteins expressed by the cell. Recent evidence suggests that these rapidly degraded peptides

*To whom correspondence should be addressed. Tel: 713 798 8993; Fax: 713 798 5075; Email: rlloyd@bcm.edu

may be produced from events where elongation is truncated (12).

Reduced ribosome processivity is caused by inappropriate chain termination, which could occur via several mechanisms. Certain types of coding sequences promote early chain termination via induction of ribosome stalling, which may increase the probability that ribosomes will release the mRNA. These include occurrences of rare codons (13), lengthy repeats of certain specific codons as in Epstein–Barr virus EBNA1 protein (e.g. Gly/Ala) (12) or stalling sequences such as the foot-and-mouth disease virus 2A (FMDV 2A) peptide that can cause cotranslational peptide scission (14,15). Alternatively, nascent peptide sequences can interact with the ribosome to modulate its elongation rate, likewise leading to slowing or stalling (16,17). When ribosomes stall in these systems, it is still unclear what proportion of stalled ribosomes recover from the event and what proportion disengage. Conversely, it is possible that some inappropriate chain termination events could be the consequence of inherently poor ribosome processivity. Mutations in ribosomal components can alter processivity (18), suggesting that the ribosome itself governs processivity to some extent.

Recently, higher order structure of polysomes in wheat germ has been linked to increased translation rates (19). Isolated cytoplasmic polysomes of both prokaryotic and eukaryotic origin appear as double rows of ribosomes that may result from collapsed circles when examined by transmission electron microscopy (19–22), atomic force microscopy (21) or cryo-electron microscopy (23). Strikingly, these published instances all display ribosomes associating closely with their neighbors to form double rows packed together, arranged in such a way that the 40S ribosomal subunits are interacting across the double row with 60S subunits oriented towards the outside of the polysome. In addition, free 70S ribosomes can dimerize through interactions between small subunits (24). Such double-row polysome structures may form in eukaryotic cells as a consequence of mRNA circularization via eukaryotic translation initiation factor 4G (eIF4G) binding both eukaryotic translation initiation factor 4E (eIF4E), bound to the 5′-cap, and poly(A)-binding protein (PABP), bound to the 3′-poly(A) tail (25). The double-row polysome configuration is consistent with functional postulates, such as the circularization of mRNA for efficient translation and positioning peptide exit channels away from each other to maximize space for protein folding

This study introduces a novel long, tripartite reporter RNA for measuring ribosome processivity and provides evidence that a time-dependent increase in ribosome processivity can be measured. We show that processivity is dependent on ORF length, with ribosomes completing smaller ORFs more readily and processivity increasing more robustly over time. This time-dependent increased processivity was dependent on a poly(A) tail and PABP, but was not dependent on intact eIF4G. Electron micrographic analysis of polysome structures revealed a correlation with the formation of packed ribosome structures with time that could allow inter-ribosomal cooperativity to support increased processivity.

MATERIALS AND METHODS

Plasmids

pRL-FMDV-Triple was previously made by PCR amplification of a NheI-RLuc-NotI fragment, Not I-FMDV 2A-β-galactosidase-Sst II fragment and SstII-FMDV-FLuc-ClaI fragments from plasmids pRL-HL (26), p-SV-β-galactosidase (Promega) and pRL-HL, respectively. The three PCR products were cloned into Bluescript KS+, excised with the appropriate restriction enzymes and assembled in a three-way ligation in Bluescript. The final Triple ORF region was excised with NheI and ClaI and cloned into similarly digested pRL-HCV-FLpA (27). The pG series of plasmids was created from pGEA30 that contains the 3′-terminal 269 coding nucleotides and the 3′-UTR (untranslated region) from poliovirus appended to a 30-nt polyA region, inserted into the XbaI and HindIII sites of pGEM-T Easy (Promega). The pGEA30 transcript was shortened by amplifying the desired section of the plasmid with 5′-phosphorylated primers and ligating the product (upstream primer 5′-TTC TAG AAT GAA TCA CTA GTG AAT TCG CG, downstream primer 5′-TAG TAA CCC TAC CTC AGT CGA ATT GG). This intermediary plasmid was mutagenized to place an AgeI restriction site at the 3′-end of the synthetic poly(A) tail (sense primer 5′-AAA AAA AAA AAA AAA AAA ACC GGT TCG AGC TCG CCC GGG GAT C, antisense primer 5′-GAT CCC CGG GCG AGC TCG AAC CGG TTT TTT TTT TTT TTT TTT T). The resulting plasmid was digested with EcoRI and then religated to reverse the promoter usage of the plasmid. The resulting plasmid, pGT7, was digested with XbaI. The coding region of Triple was amplified from pRL-FMDV-Triple, adding SpeI restriction sites on each end of the product (forward primer 5′-CCA ACT AGT ATG ACT TCG AAA GTT TAT GAT CCA GAA CAA AGG, reverse primer 5′-CCA ACT AGT TTA CAA TTT GGA CTT TCC GCC CTT C). The PCR product was digested with SpeI and ligated into pGT7 backbone digested with XbaI. Insert orientation was determined by sequencing. pG-Triple-Δsmall was created by digestion of pG-Triple with HpaI and ligation of the backbone. pG-Triple-Δfs was created by digestion of pG-Triple with BsmBI and AleI and ligation of the backbone. pG-Triple-Δβ-gal was created serendipitously during a purported AleI digest and ligation of the resulting backbone.

In vitro transcription

pG-Triple plasmids were linearized with either AgeI [poly(A)] or BglII [no poly(A)] and purified by phenol–chloroform extraction followed by ethanol precipitation and washing. Resuspended templates were transcribed using the mMessage mMachine T7 *in vitro* transcription kit (Ambion) according to manufacturer's instructions and conditions to achieve 80% capping efficiency. Completed transcription reactions were treated with DNase I for 10 min at room temperature and then purified by phenol–chloroform extraction followed by isopropanol–NaOAc precipitation and ethanol washing.

RNAs transcribed from pG-Triple plasmids are denoted as G-Triple herein, to distinguish the RNA from the template DNA.

In vitro translation reactions

HeLa S3 cells were grown in Joklik's modified minimum essential medium (Sigma) supplemented with 1% fetal bovine serum and 9% fetal calf serum and harvested, resuspended in two pellet volumes of 20 mM HEPES pH 7.2, 10 mM KCl, 1.5 mM $MgCl_2$, Dounce homogenized and centrifuged for 10 min at 7000*g* to create translation lysate. Lysate was nucleased by incubation at 18°C for 5 min in the presence of 0.62 mM $CaCl_2$ and 2500 gel units/ml micrococcal nuclease (New England Biolabs). The reaction was quenched by the addition of 2.4 mM EGTA. *In vitro* translation reactions contained 50% (v/v) translation lysate, 2 ng/μl reporter RNA, 90 mM KOAc, 20 mM MOPS–KOH, 1 mM $MgCl_2$, 15 mM creatine phosphate, 50 ug/ml creatine kinase, 4 mM DTT, 0.5 mM ATP, 0.1 mM GTP and 0.1 mM complete amino acids. Radiolabeled translation reactions contained 1.3 mCi/ml ^{35}S-Tran label (MP Biomedicals). Luciferase activity was measured by dual luciferase assay (Promega). Under these translation conditions, denaturing gel analysis of ^{32}P-labeled RNA showed rapid loss of typically ~60% of input G-Triple or derivative G-Triple RNAs within 5–10 min of addition to lysates; however, the bulk of remaining RNA was stable through the duration of the translation reaction.

Protein purification

Coxsackievirus 2A protease was purified by ion-exchange chromatography and size-exclusion chromatography as previously described (28). GST-Paip2 was overexpressed in *E. coli* containing pGEX-6P-Paip2 (29) by induction with 1 mM IPTG and affinity purified using Glutathione Sepharose 4B (GE Healthcare). His-PABP was expressed from pET28a-PABP in *E. coli* BL21(DE3)pLysS cells by induction with 1 mM IPTG and purified using sonication, 30% ammonium sulfite precipitation of impurities and affinity purification using Ni-NTA chelating resin (Qiagen) as described previously (30).

PABP depletions

PABP was depleted from nucleased HeLa lysate by incubation of lysate at 4°C for 1 h with GST-Paip2-bound Glutathione Sepharose 4B resin (GE Healthcare) essentially as previously described (31). Briefly, Glutathione Sepharose 4B resin was incubated with GST-Paip2 overnight at 4°C and the resin was washed and incubated with nucleased HeLa lysate for 1 h at 4°C. Lysate was separated from the beads by pipetting.

Electron microscopy

Polysome fractions from HeLa cells were prepared by sedimentation of postnuclear cell lysates pretreated with cycloheximide (100 μM) through 5 ml continuous glycerol gradients (20–50%) in 15 mM HEPES pH 7.4, 100 mM KCl, 5 mM $MgCl_2$ and 0.1 mg/ml cycloheximide. Gradients were centrifuged in a SW 55 rotor at 43 000 rpm for 60 min and fractions collected with continuous UV monitoring with an ISCO Gradient Fractionator.

Polysome fractions were directly applied to formvar–carbon- or carbon-coated copper grids by floating on a 10 μl droplet on a parafilm sheet for 4 min, followed by three successive washes in water. Grids were stained with 1% uranyl acetate for 30 s, and drained and dried. Products of *in vitro* translation reactions were examined by spread technique on a hypophase of 10 mM HEPES pH 7.4, 100 mM KCl, 5 mM $MgCl_2$. Grids were briefly touched to sample spread on the hypophase, washed three times in water droplets and stained with 1% uranyl acetate. Images were obtained on a Hitachi H-7500 transmission electron microscope at ×12 000–×25 000 magnification.

RESULTS

A tripartite reporter produces multiple products from a single ORF

In order to examine both early and late ribosome transit along an ORF simultaneously, a novel tripartite reporter was constructed to produce three tandem proteins within one reading frame. pG-Triple is a template for *in vitro* translation that produces a 5.94-kb G-Triple transcript with a 76-nt 5′-UTR, a single 5750-nt ORF containing *Renilla* luciferase (RLuc), β-galactosidase (β-gal), firefly luciferase (FLuc) coding regions in tandem, an 82-nt 3′-UTR and a 30 residue poly(A) tail (Figure 1A). The β-gal coding region is flanked by modified FMDV 2A peptide sequences, which cause apparent 'scission' of the nascent peptide in *cis* (32) in cotranslational reactions involving a programmed ribosome termination/resumption mechanism. A derivative construct, pG-Triple-Δsmall, contains a 630-nt deletion in the β-gal coding region while preserving the Triple reading frame. pG-Triple-Δβ-gal contains a 2700-nt in-frame deletion, which excises the majority of the β-gal coding region. pG-Triple-Δfs contains a 2854-nt deletion in β-gal that disrupts the Triple reading frame, resulting in an out-of-frame FLuc coding region. The FMDV 2A peptide regions were inserted to allow full catalytic activity of RLuc and FLuc by deletion of fusion peptide sequences. This was not absolutely necessary to obtain efficient luciferase activity, since many fusion peptides have been reported with high luciferase activity, and we have shown that appendage of fusion sequences 5′ of FLuc had no effect on FL enzymatic activity (33). Figure 1B shows an autoradiograph of the products of G-Triple RNA produced in *in vitro* translation reactions from HeLa cell lysates. The FMDV peptide sequences produced cleaved products with high efficiency; however, unprocessed peptides larger than β-gal were produced. Translation profiles of G-Triple-Δsmall and G-Triple-Δβ-gal demonstrate that these larger peptides contain β-gal, as partial deletion of the β-gal coding region shortened the large polypeptides correspondingly. RLuc appeared as multiple bands from read-through

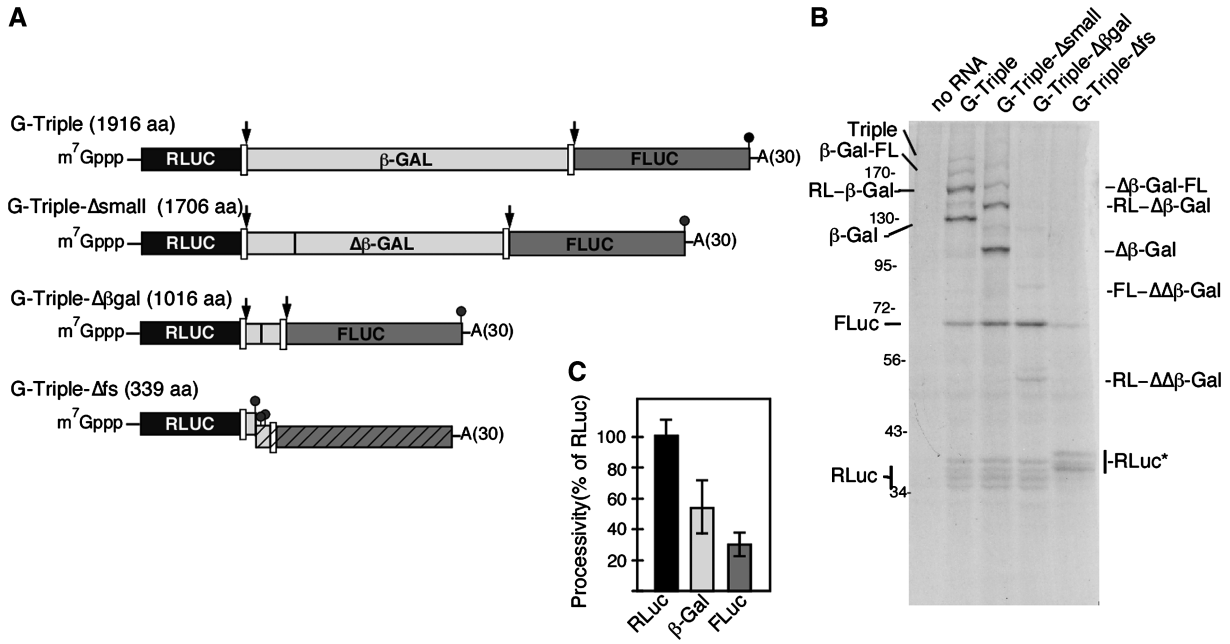

Figure 1. Triple ORF constructs. (**A**) Diagram showing coding regions and ORFs present in pG-Triple and derivative constructs. In-frame FMDV 2A peptide coding regions, denoted by white boxes, lead to scission of translated peptides at carboxyl termini denoted by arrows. Stop codons are denoted by black filled circles. (**B**) Polypeptides produced by *in vitro* translation of G-Triple RNAs in HeLa lysates. An autoradiograph of ^{35}S-Met/Cys label of translation products is shown. Products produced by full-length G-Triple RNA (second lane) are denoted on the left. Incomplete processing products produced by G-Triple-Δsmall and G-Triple-Δβ-gal RNA are denoted on the right. RLuc* indicates RLuc fusions resulting from partial elimination of FMDV 2A peptide and appendage of a short peptide from an alternate reading frame. (**C**) Densitometric quantitation of total ribosomes that complete RLuc, β-gal and FLuc ORFs. Autoradiographs from three separate 2-h translation experiments as shown in (B) were used. Bands were quantified with ImageJ. All protein products containing each of the three proteins were combined in calculations and molar ratios (ribosome transits) derived by compensating for the number of Met/Cys residues in each protein. Results are plotted as percentage of ribosomes that complete transit of each ORF, relative to RLuc (100%). Error bars indicate SD.

initiation at nearby downstream AUG codons in HeLa lysates. Such readthrough has been seen before (34), but is accentuated for unknown reasons in this construct with a longer 5′-UTR. The RLuc bands from G-Triple-Δfs are slightly larger than those produced from the other Triple RNAs as the FMDV 2A site proximal to RLuc has been destroyed in this reporter, leaving a small C-terminal tag on RLuc. G-Triple-Δfs produces FLuc at a low level despite the reporter's shifted reading frame, possibly indicative of stop codon readthrough, weak initiation on internal AUGs and/or background initiation on incomplete G-Triple-Δfs RNA fragments. Quantitation of FLuc enzymatic activity in further experiments below shows that FLuc production from G-Triple-Δfs is very low compared to the other Triple reporters (Figure 3B).

Ribosome processivity on the long Triple ORF increases exponentially over time in a poly(A)-dependent manner

We translated *in vitro* transcribed G-Triple RNA with and without a poly(A) tail in nuclease HeLa lysate to observe the kinetics of RLuc and FLuc production by luciferase assays (Figure 2A). As expected, because of the tandem arrangement RLuc activity was detected earlier than significant FLuc activity. Based on timing of appearance of luciferase activity in kinetics assays with G-Triple and monocistronic RLuc or FLuc RNAs, we estimated ribosome transit times at 5 min for the RLuc coding region and 23 min for the whole Triple ORF (data not shown). Translation of G-Triple was enhanced by the presence of a poly(A) tail and the polyadenylated transcript produced approximately four-fold higher levels of both RLuc and FLuc (Figure 2A, compare A and noA). This enhanced translation is an expected manifestation of cap-poly(A) synergy commonly observed with monocistronic RNAs (35,36) and suggests that eIF4F and PABP are efficiently interacting with Triple RNA in the system. While the production of RLuc from G-Triple followed relatively linear kinetics regardless of polyadenylation status, production of FLuc from the polyadenylated G-Triple RNA followed a distinctly nonlinear pattern, increasing exponentially over time, where production of FLuc from the nonpolyadenlyated Triple remained linear. This behavior is very unusual in an *in vitro* system, which tends to become less efficient over time, although there has been a report of translation accelerating over time on uncapped, nonpolyadenylated reporters in wheat germ extract supplemented with a continuous flow of energy (37). Furthermore, relative production of FLuc to RLuc from G-Triple was much lower than expected, scoring roughly 8-fold lower in relative light units in dual luciferase assays (Figure 2A).

This indication of low ribosome processivity was further explored by examining the ratio of luciferases being produced over time (Figure 2B). We converted the FLuc/RLuc values to a 'percent processivity' value,

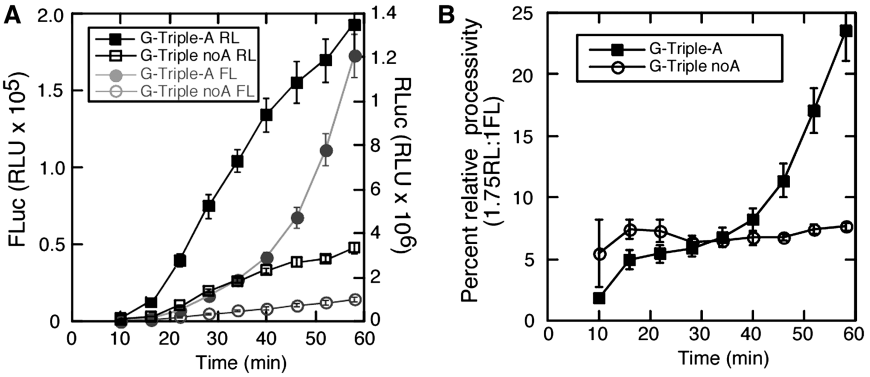

Figure 2. Triple processivity increases exponentially over time in a poly(A)-dependent manner. Nucleased HeLa lysate was pre-incubated at 35°C and then programmed with equivalent amounts of G-Triple-A and G-Triple-noA RNA for *in vitro* translation at 35°C. Dual luciferase assays were performed on aliquots of the reaction at the indicated timepoints. (**A**) Translation of G-Triple is enhanced by a poly(A) tail. (**B**) Processivity (FL/RL) of G-Triple changes over time. Percent processivity was calculated from FL/RL relative light units (RLU) by applying the conversion factor 1.75 RLuc RLU:1 FLuc RLU, which was derived based on measurements of *in vitro* translation reactions containing equal amounts of RLuc RNA and FLuc RNA. Error bars indicate SD.

estimating the percentage of initiating ribosomes that completed the Triple ORF by comparing the FLuc/RLuc ratio for the experiment to the FLuc/RLuc ratio for an *in vitro* translation reaction translating equal amounts of monocistronic RLuc RNA and monocistronic FLuc RNA (data not shown). If the processivity defect was simply due to a constant rate of ribosome drop-off before termination, the FLuc/RLuc ratio would remain constant once the first round of translation was complete as RLuc and FLuc would both be produced at separate yet constant rates. Figure 2B shows relative processivity on the nonpolyadenylated G-Triple reporter that was constant throughout the experiment. In contrast, processivity on the polyadenylated G-Triple reporter began to increase exponentially at 30 min, correlating with the nonlinear accumulation of FLuc seen in Figure 2A and continued to increase in this manner through the end of the time course. This implies that this system was not saturated even as the reporters underwent multiple rounds of translation (calculated Triple transit time is 20–25 min). The calculated processivity of the Triple ORF at 60 min varies between 10% and 25% in numerous trials, lending further evidence to this idea. Since processivity increased nonlinearly, it suggests that the processivity increase is based upon a cooperative function, where each ribosome that completes transit increases the probability of subsequent ribosomes to complete transit. The processivity increase requires a poly(A) tail and is completely absent in the nonpolyadenylated G-Triple reporter. These results suggested PABP as a probable effector of the processivity increase.

Quantitation of proteins in a series of repeat autoradiographs of translation reactions carried out for 2 h (Figure 1C) also indicated that there was a progressive loss of ribosomes completing the β-gal and FLuc ORFs; thus, not all initiating ribosomes completed elongation across the full Triple ORF. β-gal was produced at only 56% molar levels of RLuc and FLuc was produced at only 32% molar levels. Quantitation of autoradiographs of 60 and 120 min translation reactions also revealed an increase in FLuc apparent processivity, which rose from 21% to 38%, respectively (data not shown), thus generally supporting processivity data obtained with luciferase assays.

Increased ribosome processivity occurs earlier on shorter templates

The overall low processivity of G-Triple RNA was due to either the large size of the Triple ORF or the presence of the FMDV 2A sites, which cause ribosome pausing (15). To investigate this, sections of the β-gal coding region were excised from Triple to shorten the ORF length but to retain both luciferase coding regions (Figure 1A). When these truncations were compared to the full-length reporter in *in vitro* translation reactions, RLuc production from all reporters remained linear (Figure 3A). Curiously, G-Triple-Δβgal, a reporter with a large in-frame deletion removing most of β-gal from the Triple ORF, exhibited a ~60% decrease in RLuc activity despite repeated calibrations and multiple RNA preparations. FLuc production differed even more dramatically with these reporters (Figure 3B). G-Triple-Δsmall, which contains a small in-frame deletion in the β-gal coding region, produced FLuc at a similar rate to the full-length Triple, but the exponential increase in FLuc was slightly stronger, possibly reflective of the slightly shortened ORF. FLuc production from G-Triple-Δβ-gal followed markedly different kinetics; the increase in FLuc was stronger and occurred earlier than that seen with the full-length ORF, despite the decreased production of RLuc at the 5′-end of the ORF compared to the other reporters. Reactions programmed with G-Triple-Δfs, containing a large out-of-frame β-gal deletion resulting in a reading frame that ends shortly after the RLuc coding region, produced FLuc activity at a low, basal rate. This could reflect the integrity of the RNA used in the experiments or could partly result from ribosome reinitiation downstream of the stop codon and stop codon readthrough. When these results are plotted as processivity over time (Figure 3C), it becomes obvious that while G-Triple-Δfs

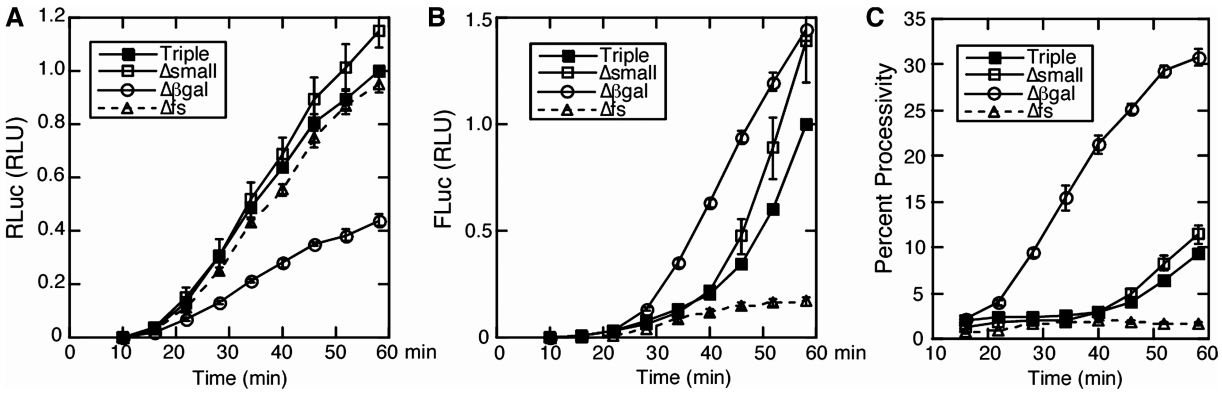

Figure 3. Shorter ORFs exhibit increased processivity and greater cooperativity. G-Triple, G-Triple-Δsmall, G-Triple-Δβ-gal and G-Triple-Δfs were translated in nucleased HeLa lysate as described in Figure 2. Note that RNA names are shortened in legends. (**A**) Production of RLuc from the Triple RNA variants is largely uniform. (**B**) Production of FLuc from the Triple RNA variants increases with decreased ORF size. (**C**) Percent processivity on Triple variants is higher on shorter ORFs. Error bars indicate SD.

processivity remains very low due to the lack of in-frame FLuc production and G-Triple-Δsmall processivity closely matches that of the full-length Triple, processivity of G-Triple-Δβ-gal increases dramatically early in the reaction (20 min compared to 40 min for full-length Triple). Taken together, shorter ORFs correlated with stronger and faster increases in processivity.

PABP is required for exponential increase in FLuc production

After observing that a nonpolyadenylated Triple RNA did not exhibit an exponential increase in ribosome processivity over time (Figure 2B), we sought to recapitulate these results by performing translation reactions in the absence of PABP. PABP-interacting protein 2 (Paip2), which binds PABP and releases it from poly(A) tails (38), has been used previously to deplete PABP from nucleased lysate with minimal depletion of other PABP-interacting factors such as eIF4G (31). PABP was depleted from nucleased HeLa lysate with 90% efficiency (Figure 4A). When PABP was depleted, production of RLuc from G-Triple was inhibited ~80% compared to the mock-depleted lysate (Figure 4B), a similar result to that obtained previously using conventional monocistronic reporters (31) and consistent with the fact that PABP is a translation initiation factor (39,40). Addition of 10 ng/μl of recombinant His-PABP to the depleted lysate restored production of RLuc to ~50% of control levels. Conversely, FLuc production in PABP-depleted lysate was unchanged from controls through 45 min, but remained completely linear and failed to display increased translation rate of the control lysate (Figure 4C). When PABP was restored in the depleted lysate, RLuc production was partly rescued. More importantly, the restored reaction partially rescued the exponential increase in FLuc production observed in the control reaction. When processivity was examined, depletion of PABP scored as a linear increase in relative FLuc processivity from the earliest timepoints even though the actual FLuc translation rate never changed. This was mostly because RLuc translation underwent a modest but steady decrease in translation rate, while the FLuc translation rate remained linear (Figure 4D). However, both undepleted lysates and PABP restored lysates displayed very similar processivity curves, each with exponentially increased processivity occurring at late timepoints as FLuc translation rates increased.

Time-dependent increase in FLuc translation is not dependent upon intact eIF4G

Since PABP was required for the time-dependent increase in FLuc translation, we decided to test if eIF4G or eIF4E/cap function was also required. Coxsackievirus 2A proteinase ($2A^{pro}$) cleaves eIF4GI and eIF4GII very rapidly *in vitro*, >50% within 2 min, and to completion by 5 min (Figure 5A). eIF4G cleavage strongly inhibits *de novo* of cap-dependent translation by limiting mRNA–ribosome binding (41,42). When *in vitro* translation reactions were pretreated with $2A^{pro}$, RLuc production from G-Triple RNA was strongly inhibited, though a low level of translation persists and continues at a constant rate for 60 min (Figure 5B). This minimal translation activity is supported by the C-terminal eIF4GI cleavage fragment that binds eIF3 and eIF4A and can sustain a lower level of translation on capped RNA (43,44). Addition of $2A^{pro}$ at 15 or 30 min resulted in the inhibition of RLuc production after a delay, ~17 min after protease treatment, which is longer than the time required for eIF4G cleavage and RLuc ORF transit. Further, there was less impact of $2A^{pro}$ on RLuc translation rates when more time was allowed for ribosomes to load on G-Triple (Figures 5B and 8), e.g. when $2A^{pro}$ was added 30 min after translation initiated. This result parallels previous reports on monocistronic RNA translation showing decreased impact of $2A^{pro}$ addition or cap analog addition after polysome formation was achieved (30,45).

Surprisingly, addition of $2A^{pro}$ at 15 or 30 min had no effect on FLuc production that continued to increase exponentially even after production of RLuc from the 5′-end of the ORF had been inhibited (Figure 5C). As before, the overall amount of FLuc translation was low, about eight-fold lower than initial RLuc translation (data not

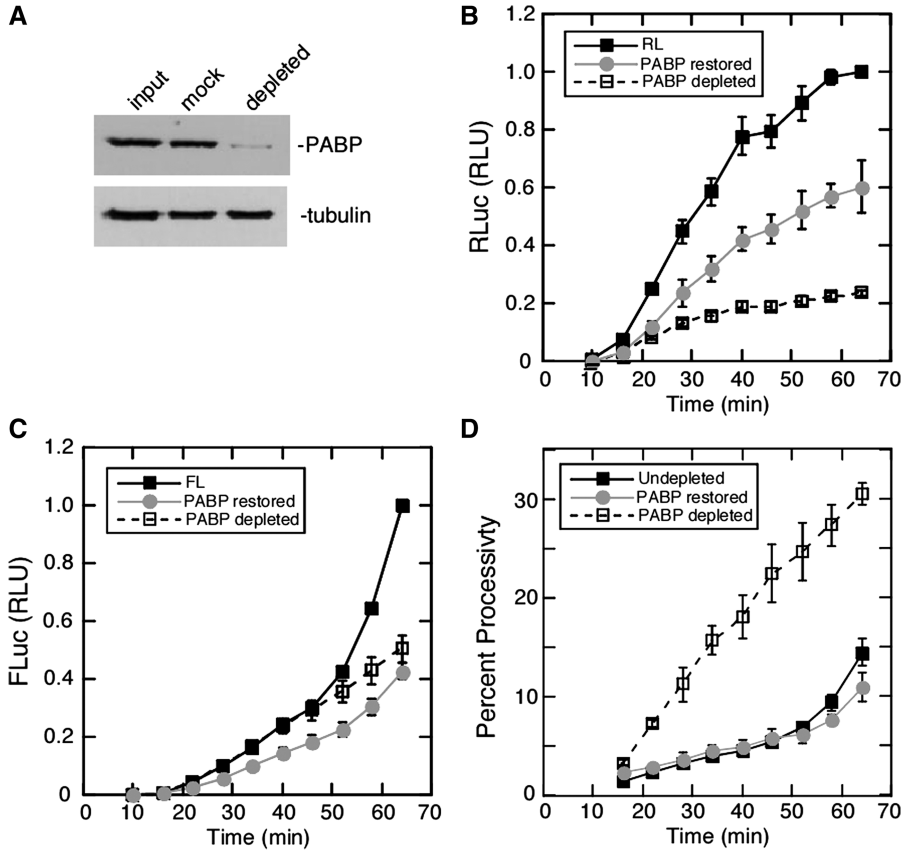

Figure 4. PABP confers cooperativity on the Triple ORF. Polyadenylated G-Triple-A was translated in nucleased HeLa lysate as described in Figure 2. (**A**) Paip2 depletes PABP from HeLa lysate. Depletions were performed using GST-Paip2 and glutathione beads as outlined in the 'Materials and Methods' section. (**B**) RLuc production from G-Triple-A in nucleased HeLa lysate, nucleased HeLa lysate depleted of PABP and depleted lysate supplemented with 10 ug/μl PABP. (**C**) Production of FLuc from G-Triple-A in nucleased HeLa lysate, nucleased HeLa lysate depleted of PABP and depleted lysate supplemented with 10 ug/μl PABP. (**D**) Percent processivity calculated from FLuc/RLuc ratios of data from (B) and (C). Error bars indicate SD.

shown). Pretreatment with $2A^{pro}$ caused an initial stimulation in low eIF4G-independent FLuc translation rate that then declined with time. This may be due to stimulation of aberrant non-eIF4F-mediated initiation or a weak cryptic internal ribosome entry site (IRES) located internally in Triple RNA that has activity when no ribosomes are transiting the region (further evidence for this is presented below).

When $2A^{pro}$ was added to nonpolyadenylated G-Triple RNA, similar results were obtained. Again, addition of $2A^{pro}$ at 15 or 30 min reduced RLuc translation rates, but not to levels observed with $2A^{pro}$ pretreatment. Similar, but slightly shorter 12–14 min lag times were observed for shifts to lower translation rates on the 5′-RLuc ORF (Figure 5D). Addition of $2A^{pro}$ at 15 or 30 min did not have a significant effect on FLuc translation through the 60 min time course of the experiments, although, as previously noted, production of FLuc from nonpolyadenylated G-Triple RNA was linear, not exponential (Figure 5C). Overall FLuc production was very low in these experiments on the poly(A)-minus RNA, comparatively only 12% of the FLuc production from polyadenylated G-Triple RNA at 60 min.

Next, the shorter G-Triple-Δβ-gal reporter, which has a calculated ORF ribosome transit time of ~13 min, was tested in $2A^{pro}$ inhibition experiments. With this reporter RLuc translation inhibition by $2A^{pro}$ began noticeably earlier, at ~10 min after protease addition versus 17 min for the full-length Triple (Figure 6A). FLuc translation inhibition by $2A^{pro}$ was observed on G-Triple-Δβgal; however, it occurred ~27 min after protease treatment (Figure 6B). This was in contrast to the complete lack of FLuc inhibition seen with the full-length G-Triple (Figure 5C). The disparity in the amount of time (10 versus 27 min) needed for $2A^{pro}$ to inhibit RLuc and FLuc on G-Triple-Δβ-gal is likely a reflection on their relative positions on the ORF. RLuc, at the 5′-end of the ORF, registers the effects of translation initiation inhibition more quickly since most enzymes are produced as a result of cap-dependent *de novo* initiation rather than any potential 3′–5′ ribosome reinitiation reactions. Production of FLuc from the reaction pretreated with $2A^{pro}$ was negligible (Figure 6B), possibly indicating that a prospective cryptic weak IRES element in the β-gal coding region postulated above has been excised.

Inhibition of eIF4E-cap interaction does not block enhanced FLuc production

To inhibit cap-dependent initiation with another approach, we added excess cap analog to translation

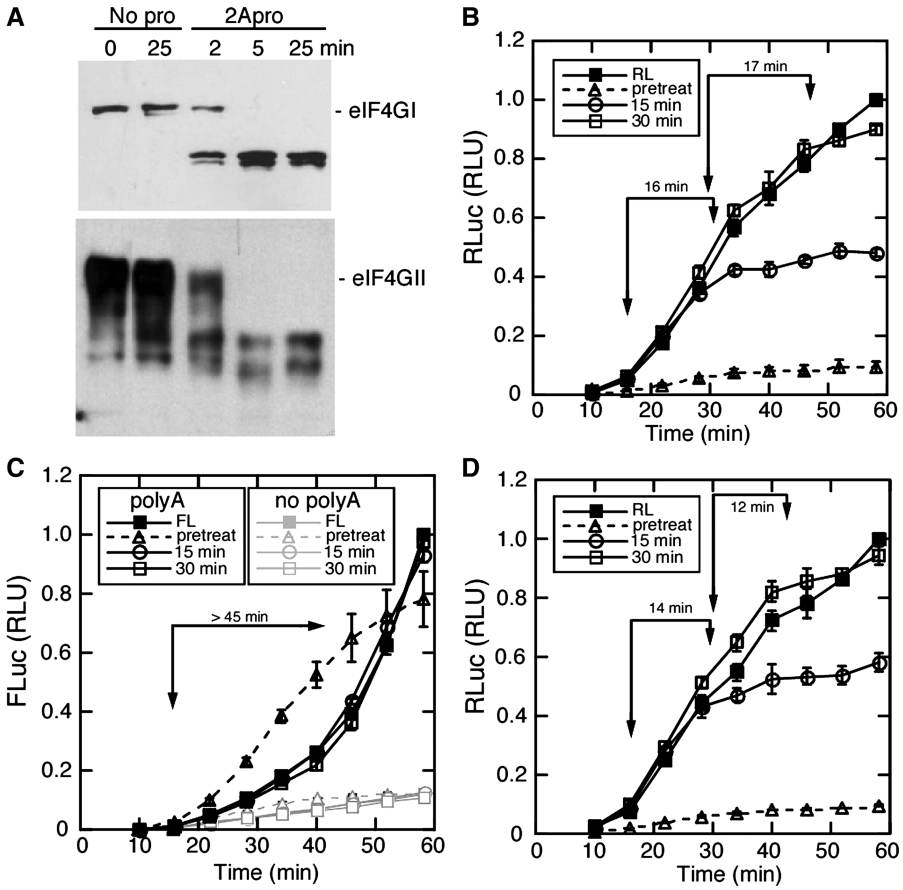

Figure 5. Triple RLuc, but not FLuc, production is inhibited by addition of $2A^{pro}$ *in vitro*. (**A**) Immunoblots showing cleavage of eIF4GI and eIF4GII by addition of 2A protease. Lysates incubated without protease (no pro) are on the left. (**B**) RLuc production from G-Triple-A. Equivalent amounts of G-Triple-A RNA were added to nucleased HeLa lysate and incubated for the indicated time at 35°C. Lysates were pre-incubated for 5 min at 35°C prior to start of the translation reaction with or without $2A^{pro}$ as indicated. Protease was added at 15 or 30 min. RLUs were normalized to maximum control translation for each reporter except (**C**) where RLU from both reporters was normalized to G-Triple-pA control. Arrows denote time span after $2A^{pro}$ addition before translation rate was affected. (C) FLuc production from pG-Triple-A RNA (black lines) and G-Triple-noA (gray lines). (**D**) RLuc production from G-Triple-noA RNA. Error bars indicate SD.

reactions at different timepoints. The effect of cap analog inhibition on *de novo* RLuc translation was similar to the effect of eIF4G cleavage and previous exogenous cap inhibition studies using a conventional reporter (45); however, decline in translation rate was observed earlier, ~7–8 min after addition of inhibitor (Figure 7A). The effect of cap analog on FLuc production was also similar to the effect of eIF4G cleavage, but not identical. Most notably, addition of inhibitor after ribosomes had loaded the template did not block the time-dependent increase in FLuc translation and processivity (Figure 7B). Also, addition of cap analog after ribosomes loaded (15 min) caused the increase in FLuc translation processivity to occur earlier. This is consistent with eIF4E–cap interaction playing a modest role inhibiting the time-dependent increase in processivity. While cap analog did not block the increase in processivity, it may decrease its duration. When inhibitor was added at 15 min, a gradual decrease in FLuc translation rate began to occur after a 30-min delay. Similar to $2A^{pro}$, pretreatment of lysate with cap analog initially caused a weak stimulation of anomalous cap-independent FLuc production that decreased with time.

$2A^{pro}$ and cap analog produced unexpected effects that warranted further analysis of translation rates resulting from inhibitor additions. Figure 8 shows that when inhibitor was added to G-Triple translation reactions at 15 min, when ribosomes had completed three-fourth the transit of the ORF, RLuc translation rates at the 5′-ORF adopted new levels that were near 15–20% of control rates. This was significantly higher than translation resulting from pretreatment. If ribosomes were allowed to load for 30 min, inhibitors only dropped translation rates to levels of 22–29% of control. The exception was G-Triple-Δβ-gal RNA, which was affected more drastically by $2A^{pro}$; however, both late inhibitor additions failed to reduce RLuc translation to the minimum rates achieved by pretreatment. These results are consistent with a fraction of preloaded ribosomes recycling from 3′- to 5′-ends of RNA in an eIF4F-independent manner.

Time-dependent increase in ribosome interactions on Triple RNA

Recently in bacterial and wheat germ systems double-row polysome structures with closely interacting ribosomes

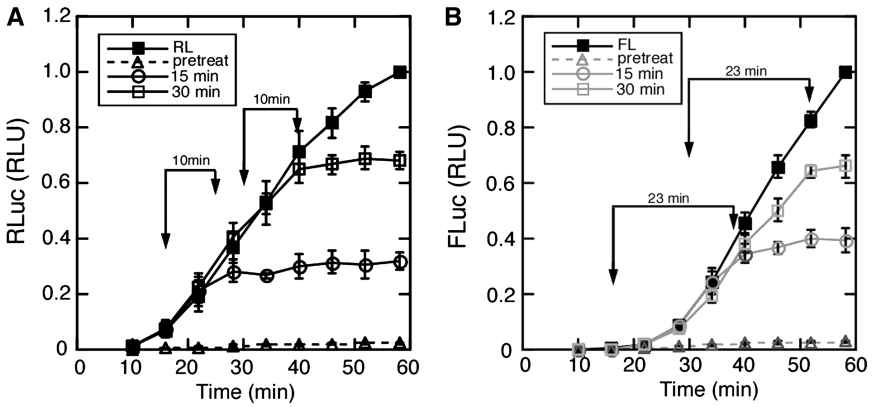

Figure 6. TripleΔβ-gal loses processivity and cooperativity after addition of $2A^{pro}$. G-Triple-Δβ-gal RNA was translated in nucleased HeLa lysate treated with $2A^{pro}$ at the indicated timepoints as in Figure 5. (**A**) Production of RLuc from G-Triple-Δβ-gal RNA. (**B**) Production of FLuc from G-Triple-Δβ-gal. Error bars indicate SD.

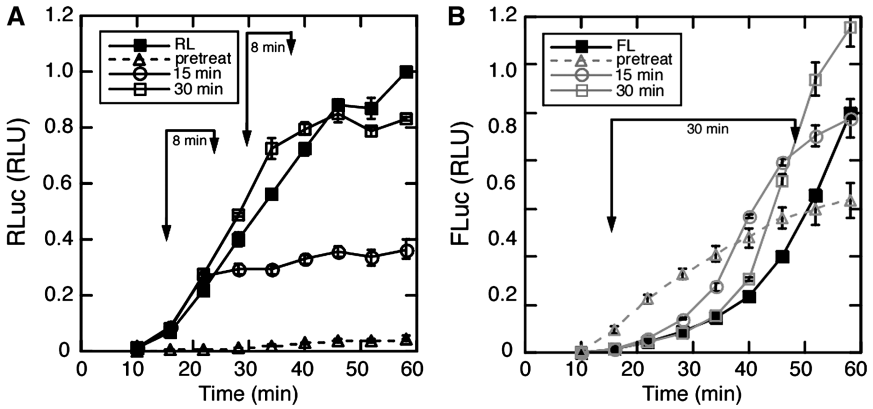

Figure 7. Exogenous cap does not block FLuc production from Triple RNA. Polyadenylated G-Triple RNA was translated in nucleased HeLa lysate that was pre-incubated for 5 min at 35°C with or without 1 mM cap analog. The 1-mM cap analog was added to reactions at indicated timepoints. (**A**) Production of RLuc from G-Triple-A. (**B**) Production of FLuc from G-Triple-A. Error bars indicate SD.

were observed to form, in which small ribosomal subunits interact and are arranged along the interior of the structure. Similar structures also formed *in vitro* in translation reactions with both systems (19,23). To determine whether similar structures could form with human polysomes, we performed electron microscopy on isolated polysome fractions from cells and *in vitro* translation lysates. Figure 9A and B shows images of polysome structures isolated from HeLa cells. Samples were taken from glycerol gradients in the deeply sedimenting large polysome region. Some structures appeared as disordered grape-like clusters that were reported decades ago; however, a large proportion were in predominantly double-row arrangements similar to those reported in wheat germ (arrows) (19,20,46). This arrangement was more apparent in polysomes containing more than six ribosomes. To determine if such structures form in HeLa translation lysates, comparative translation of FLuc RNA was carried out in each system and ribosomes examined by electron microscopy. Before translation began, ribosomes were observed to be completely disordered (data not shown), but by 30 min of translation time, some ribosomes were observed arranged in tetramers, hexamers and occasionally larger double-row arrangements in both wheat germ and HeLa translation lysates (Figure 9C and D). In addition, wheat germ lysates displayed apparent short strings of single ribosomes that were packed tight enough to potentially allow interaction (arrowheads) and contained a higher density of double-row structures than HeLa lysates. By 60 min of translation, structures with packed ribosomes were observed to be larger and more numerous in both systems; however, HeLa lysates were not as efficient in producing packed structures, nor were they as ordered (Figure 9E and F). The translation efficiency of the wheat germ lysate determined by luciferase activity was approximately five-fold higher than that of HeLa lysates at all timepoints, likely demonstrating a significantly higher initiation rate (data not shown). When translation of G-Triple RNA was examined, ribosomes were commonly arranged in single rows, but often the spacing was wider than 20 nm or more, especially in the HeLa lysate (Figure 9G and H, arrowheads). The density of single-ribosome packing increased with time. Organization into small double-row structures of 4–6 ribosomes was observed, but the frequency of these structures was much lower and delayed in appearance compared to FLuc translations, requiring 45 min to be observed at all (data not shown). Further, the organization of double-row

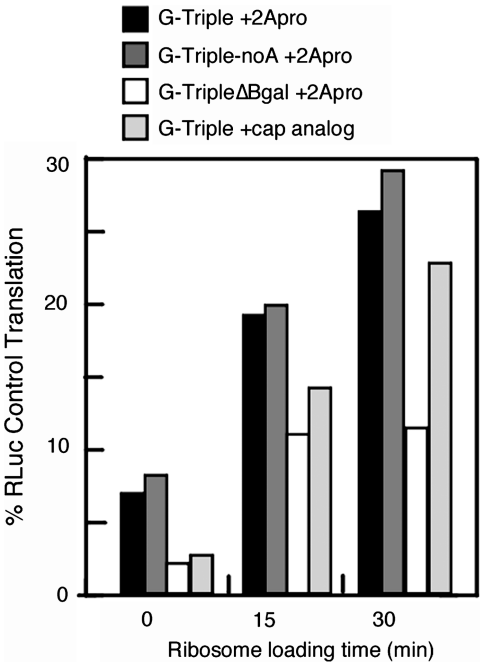

Figure 8. eIF4F inhibitors display incomplete impact when added after polysome loading. Translation rates of RLuc (slopes) were calculated at various times after addition of inhibitors had driven translation to new rates in experiments shown in Figures 5–7. The values are expressed relative to the translation rate of RLuc in control reactions with no inhibitor.

structures was not observed to attain the same size or order seen on FLuc templates (Figure 9G and H). Taken together, the frequency of attainment of large ordered double-row structures correlated with high translation initiation rate and shorter ORFs, and occurred significantly sooner on shorter RNAs.

DISCUSSION

To our knowledge, this is the first report demonstrating that ribosome processivity, the probability of a ribosome completing a given ORF, changes over time. A recent report of acceleration of translation was linked to accumulation of ribosomes on RNAs with time in a wheat germ system; however, this assay could not differentiate between increased translation initiation and increased ribosome retention (37). The unique nature of G-Triple RNA helped to reveal changes in processivity due to its ability to report ribosome transit on 5′-and 3′-regions of the ORF independently, coupled with its very long length, which reduced overall ribosome processivity enough that increases in FLuc production rates at the 3′-end of the ORF could be measured. It is likely that inclusion of two FMDV peptide coding regions, which cause peptide 'scission' in conjunction with a ribosome pausing mechanism (14,15), also contributed to the low processivity of G-Triple.

Although the mechanism that supports time-dependent increased processivity is not yet known, several determinants were identified. First, the increased processivity required a poly(A) tail in these assays. Second, PABP was required, and it partly restored the time-dependent processivity increase when added back to depleted translation reactions. Third, the increased processivity occurred more robustly and more quickly on shorter templates in conjunction with higher initial processivity and reduced ORF transit time. Finally, the increased processivity was independent of blockage to *de novo* initiation with $2A^{pro}$ or cap analog to a point; severe restriction of *de novo* initiation by cap analog showed a modest decrease in FLuc production after a 30-min delay (Figure 7B), and $2A^{pro}$ could decrease FLuc translation only on the shortest RNA tested, after a 23-min delay (Figure 6C). These data suggest that the increased processivity phenotype does not require intact eIF4G, and any eventual decline in the FLuc production rate requires about two complete successive rounds of ribosome transits. It is possible that inhibitory effects from eIF4G cleavage may occur on full-length G-Triple at later timepoints than were measured (e.g. 70–80 min), after a similar number of complete ribosome transits have occurred.

Experiments that blocked eIF4F function revealed several unexpected results incompatible with a scenario, where all ribosome loading occurs in a strictly cap-dependent 5′ *de novo* initiation mechanism. First, pretreatment of *in vitro* translation reactions with $2A^{pro}$ or cap analog before addition of G-Triple seemed to stimulate transit on the FLuc coding region by 15 min (Figures 5 and 7). This is most consistent with some ribosomes loading internally at a weak cryptic IRES. This function was not observed if ribosomes were allowed to load RNA for 15 min before protease or cap analog was added, suggesting that transiting ribosomes destroyed an IRES secondary structure. This structure, if it actually exists, does not impact on the mechanism driving increased processivity, which still occurred if ribosomes were preloaded on RNA before inhibitor was added. A second unexpected result from blocking eIF4F function was observed at the 5′-RLuc ORF. Surprisingly, the time required to reduce RLuc translation was dependent on RNA length, taking 17 min on G-Triple and only 10 min on the shorter G-Triple-Δβ-gal RNA. Both RNAs have identical 5′- and 3′-UTRs. In these reactions, most eIF4G was cleaved in 2 min and all were cleaved by 5 min. We note that the inhibition time for each RNA (17 versus 10 min) was similar to the calculated ORF transit time for each (20 versus 12 min). This result links kinetics of translation inhibition at the 5′-ORF to the ribosome transit time, suggesting that some ribosomes may recycle from 3′- to 5′-ends of the RNA and extend the duration of translation after inhibition of eIF4F occurs. A third unexpected observation was that the magnitude of RLuc translation inhibition resulting from eIF4G cleavage became less drastic when the longer ribosomes were allowed to load the RNA template (Figure 8). The $2A^{pro}$ always had an effect on RLuc production, but this lessened with time so that if ribosomes were allowed to translate for 30 min, $2A^{pro}$ only reduced translation rates by 72%. This contrasts with the 93% inhibition if $2A^{pro}$ pretreatment was used. This delay and resistance to complete translation inhibition at the 5′-end of the RNA may be partly dependent on a poly(A) tail since the delay

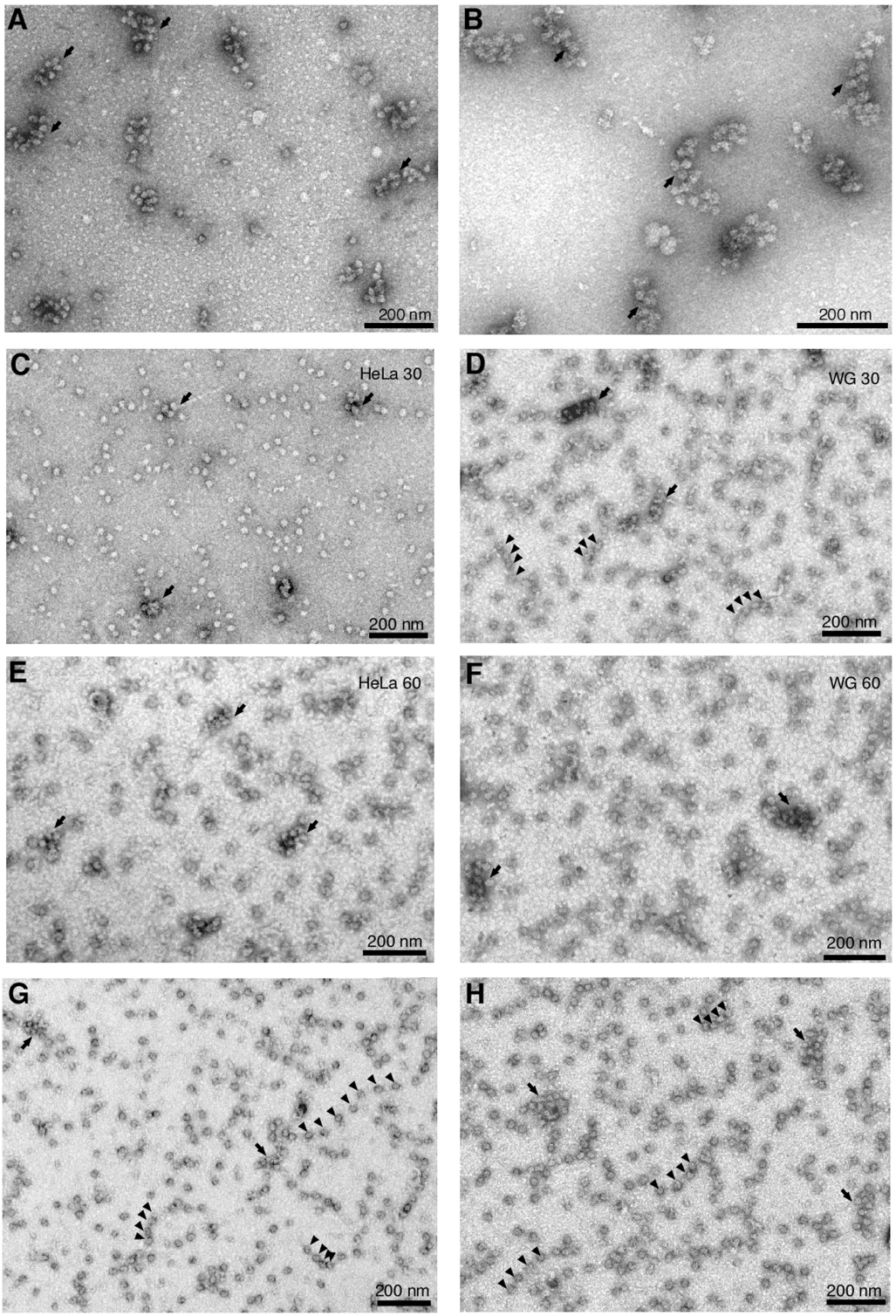

Figure 9. Polysome structure accumulates in *in vitro* translation reactions over time. (**A**, **B**) Polysomes were isolated from HeLa S3 cells by ultracentrifugation on sucrose density gradients and prepared for transmission electron microscopy by mounting via spread technique and negative staining with uranyl acetate. Double-row polysome structures are indicated by arrows. *In vitro* translation reactions originating from HeLa cells (**C**, **E** and **G**) or wheat germ (**D**, **F** and **H**) were mounted by spread technique and stained with uranyl acetate. Arrows denote ribosome tetrads or larger groups up to double-row polysomes and arrowheads denote linearly arranged ribosomes. Lysates were programmed with capped, polyadenylated FLuc RNA for 30 min of translation (C, D) or 60 min of translation (E, F). Total FLuc accumulated was $6. \times 10^7$ RLU/µl in wheat germ and 2.2×10^6 RLU/µl in HeLa lysates at 60 min. In panels (G) and (H), translation lysates were programmed with capped, polyadenylated G-Triple RNA for 60 min of translation. Total RLuc accumulated was 7.1×10^6 RLU/µl in wheat germ and 3.1×10^6 RLU/µl in HeLa lysates at 60 min.

time shortened from 17 to 12–14 min on the G-Triple-noA template. However, these results are consistent with preloaded ribosomes contributing to translation via recycling from stop codons on the same template in a mechanism that does not require intact eIF4G.

Why does $2A^{pro}$ inhibit FLuc on short G-Triple-Δβ-gal RNA but not G-Triple? One hypothesis is that an initial low ribosome processivity is required to observe subsequent organization of ribosome cooperativity that raises translation rates and that ribosome cooperativity is linked to facilitated ribosome recycling from stop to start codons. With G-Triple RNA, only ~12% of initiating ribosomes complete FLuc, which is near the threshold of maximum translation inhibition that eIF4G cleavage imposes on RLuc (Figure 5B). Thus, $2A^{pro}$/eIF4G cleavage does not inhibit translation drastically enough to choke off the input flow of *de novo* initiating ribosomes plus recycling ribosomes in this case. The shorter G-Triple-Δβ-gal RNA displayed raw RLuc and FLuc values indicating a higher proportion of ribosomes completed the FLuc ORF (~24%), which was above the threshold where eIF4GI cleavage can have a significant effect. In this case, the time delay of FLuc translation inhibition was significant, consistent with two complete ORF transits by ribosomes.

Increased processivity can be explained by an increase in cooperativity between ribosomes or associated factors that help to keep transiting ribosomes from leaving the template. The results in this study suggest the increase in FLuc processivity correlates most closely with events linked to PABP and ribosomes reaching termination codons, possibly involving interaction between PABP and eRF3 (47,48). PABP is in a unique position to interact with both initiation and termination factors including eIF4B (49), eIF4G (50), and Paip1 (51). Recent studies have shown that ribosome recycling at termination codons has distinct biochemical requirements involving eIF3 and ABCE1, the latter of which interacts with both initiation and termination factors (1,2). Also, an increased ordering of contacts and packing between ribosomes forming double-row structures was described in wheat germ that may provide such a mechanism (19). We examined native polysomes in HeLa lysates by electron microscopy and noted that a significant fraction of the polysomes maintained a similar double-row structure. When ribosomes in translation lysates were examined by electron microscopy, a similar structure was observed to form in both HeLa and wheat germ lysates on FLuc RNA, though the wheat germ translated more efficiently and produced these structures more readily. Interestingly, when G-Triple RNA was translated, polysome organization also increased with time, but did not achieve the higher level of large double-row structures observed with shorter FLuc templates within 60 min. We also observed a two-stage organization, where ribosomes were compressed linearly in single-row structures early, and tetrads and double-row structures appeared later. This temporal arrangement was especially noticeable in G-Triple translations. Further, we observed that all ribosome compaction and organization took place more efficiently on shorter templates, possibly correlating with more ribosomes encountering termination events on stop codons over the period of assay.

Taken together, the increase in FLuc processivity and increased ribosome organization both correlated with cumulative numbers of ribosomes encountering termination codons. A cooperativity mechanism based on PABP-associated factors that function at termination and promote 40S ribosome–ribosome interaction, particularly in conjunction with ribosome recycling, could be relatively independent of cap and eIF4F functions once initiated. We envision one model where 5′–3′ interaction and looping of 5′- and 3′-UTRs by initiation factors places start and stop codons in close proximity (52). Termination events would promote ribosome interactions that build cooperativity in two ways. First, proximity of 5′- and 3′-ends promotes interactions between terminating and initiating ribosome 40S subunits. Secondly, termination events requiring interaction of PABP and eRF3 may cause sufficient ribosome pausing such that the adjacent ribosome may collide with the terminating ribosome. In this model, the initial ribosome tetrad formation involves initiating and terminating ribosomes at the 5′–3′ junction, which then builds larger cooperative ribosome structures progressively towards the center of the ORF, collapsing the mRNA loop. This model dictates that the ribosome itself is regulated by the presence of other ribosomes; binding of other ribosomes could be construed as analogous to the recruitment of processivity factors. It is also possible that discrete, unidentified processivity factors exist that are recruited to or activated by the formation of such polysomes, or that facets of the known translation machinery are being modified in a way to encourage processivity as the polysome forms. Consistent with the increased ribosome cooperativity model, mathematical modeling of prokaryotic translation suggests that the elongation rate on a given ORF accelerates as coverage of the ORF by ribosomes increases, with the translation rate reaching its maximum at 95% ORF coverage (53).

Recently Kopeina *et al.* (19) showed that with a constant influx of energy, translating ribosomes nucleate into quartets and then add moieties and elongate into full double-row structures over time. Processivity in this system was not determined. These authors used kinetic analysis to examine incorporation of free radiolabeled ribosomes into polysomes and found that a given ribosome is retained in the full polysome for five rounds of translation—essentially, a terminating ribosome has an 80% chance of being reused in the polysome. Thus a 3′ to 5′ recycling mechanism may be integral to this ribosome cooperativity. This would be consistent with the observed delays we observed in translation inhibition in both RLuc and FLuc on G-Triple RNA after cleavage of eIF4G. We have previously observed similar delays on FLuc RNA (30), which were also consistent with an early report indicating that application of cap analog only weakly inhibited translation after polysomes formed (45). Interestingly, strong interactions between ORFs and 3′-UTRs of mRNA have also been observed, which may play a role in these processes (54).

Genomewise analyses of polysomes have revealed that the ribosome density of long ORFs is lower than that of

short ORFs in *S. cerevisiae* (5). It has been postulated that this is due to lower initiation rates on longer ORFs, not incomplete processivity (6). Deep sequencing of ribosome positioning on *S. cerevisiae* mRNA revealed that ribosome density is higher on the first 30–40 codons of a given ORF and declines to a uniform density through the remainder of the ORF; but the authors could not differentiate between acceleration of elongation or incomplete processivity as a cause (7). Our data in this study are consistent with deep sequencing results showing increased ribosome density near the 5′-ends of ORFs.

Imperfect translation elongation that improves rapidly after translation start fits well with current literature about the origin of major histocompatibility complex class I display peptides. A large minority of newly synthesized peptides are immediately degraded, and this pool is the main source of peptides for display by major histocompatability complex (MHC) class I molecules (8,55). This fraction of rapidly degraded peptides could be populated by incomplete peptide products originating from fresh mRNAs that are beginning to be translated. The proposed purpose of these rapidly degraded peptides is to provide display peptides for MHC class I molecules at earliest phases of viral infection. Inherent low processivity would allow translation on each mRNA to undergo a survey phase, where peptides are delivered to the immune system to vet them as self or nonself. Processivity would increase quickly to a sustained production phase, where proper gene products would be synthesized. If inter-ribosome contacts that promote cooperativity do, in fact, occur, these contacts could become more extensive over a longer ORF, helping to overcome the difficulty inherent in synthesizing large peptides to the point where even very large proteins could be produced.

ACKNOWLEDGEMENTS

The authors thank Dr L. Reineke for critical review of the manuscript, Dr P. Younan and Dr C. Rivera for technical assistance, Dr N. Sonenberg for anti-eIF4GII antiserum and Dr Y. Svitkin for the pGEX-6P-Paip2 construct.

FUNDING

National Institutes of Health grants (grant numbers GM59803 and AI50237 to R.E.L.). Funding for open access charge: Grant funding from NIH grant (AI50237).

Conflict of interest statement. None declared.

REFERENCES

1. Pisarev,A.V., Skabkin,M.A., Pisareva,V.P., Skabkina,O.V., Rakotondrafara,A.M., Hentze,M.W., Hellen,C.U. and Pestova,T.V. The role of ABCE1 in eukaryotic posttermination ribosomal recycling. *Mol. Cell*, **37**, 196–210.
2. Pisarev,A.V., Hellen,C.U. and Pestova,T.V. (2007) Recycling of eukaryotic posttermination ribosomal complexes. *Cell*, **131**, 286–299.
3. Jackson,R.J., Hellen,C.U. and Pestova,T.V. (2010) The mechanism of eukaryotic translation initiation and principles of its regulation. *Nat. Rev. Mol. Cell. Biol.*, **11**, 113–127.
4. Tsung,K., Inouye,S. and Inouye,M. (1989) Factors affecting the efficiency of protein synthesis in Escherichia coli. Production of a polypeptide of more than 6000 amino acid residues. *J. Biol. Chem.*, **264**, 4428–4433.
5. Arava,Y., Wang,Y., Storey,J.D., Liu,C.L., Brown,P.O. and Herschlag,D. (2003) Genome-wide analysis of mRNA translation profiles in Saccharomyces cerevisiae. *Proc. Natl Acad. Sci. USA*, **100**, 3889–3894.
6. Arava,Y., Boas,F.E., Brown,P.O. and Herschlag,D. (2005) Dissecting eukaryotic translation and its control by ribosome density mapping. *Nucleic Acids Res.*, **33**, 2421–2432.
7. Ingolia,N.T., Ghaemmaghami,S., Newman,J.R. and Weissman,J.S. (2009) Genome-wide analysis in vivo of translation with nucleotide resolution using ribosome profiling. *Science*, **324**, 218–223.
8. Schubert,U., Anton,L.C., Gibbs,J., Norbury,C.C., Yewdell,J.W. and Bennink,J.R. (2000) Rapid degradation of a large fraction of newly synthesized proteins by proteasomes. *Nature*, **404**, 770–774.
9. Wheatley,D.N., Giddings,M.R. and Inglis,M.S. (1980) Kinetics of degradation of ''short-'' and ''long-lived'' proteins in cultured mammalian cells. *Cell Biol. Int. Rep.*, **4**, 1081–1090.
10. Turner,G.C. and Varshavsky,A. (2000) Detecting and measuring cotranslational protein degradation in vivo. *Science*, **289**, 2117–2120.
11. Chuang,S.M., Chen,L., Lambertson,D., Anand,M., Kinzy,T.G. and Madura,K. (2005) Proteasome-mediated degradation of cotranslationally damaged proteins involves translation elongation factor 1A. *Mol. Cell. Biol.*, **25**, 403–413.
12. Cardinaud,S., Starck,S.R., Chandra,P. and Shastri,N. (2010) The synthesis of truncated polypeptides for immune surveillance and viral evasion. *PLoS ONE*, **5**, e8692.
13. Varenne,S., Buc,J., Lloubes,R. and Lazdunski,C. (1984) Translation is a non-uniform process. Effect of tRNA availability on the rate of elongation of nascent polypeptide chains. *J. Mol. Biol.*, **180**, 549–576.
14. Doronina,V.A., Wu,C., de Felipe,P., Sachs,M.S., Ryan,M.D. and Brown,J.D. (2008) Site-specific release of nascent chains from ribosomes at a sense codon. *Mol. Cell. Biol.*, **28**, 4227–4239.
15. Donnelly,M.L., Luke,G., Mehrotra,A., Li,X., Hughes,L.E., Gani,D. and Ryan,M.D. (2001) Analysis of the aphthovirus 2A/2B polyprotein 'cleavage' mechanism indicates not a proteolytic reaction, but a novel translational effect: a putative ribosomal 'skip'. *J. Gen. Virol.*, **82**, 1013–1025.
16. Lu,J. and Deutsch,C. (2008) Electrostatics in the ribosomal tunnel modulate chain elongation rates. *J. Mol. Biol.*, **384**, 73–86.
17. Wang,Z., Gaba,A. and Sachs,M.S. (1999) A highly conserved mechanism of regulated ribosome stalling mediated by fungal arginine attenuator peptides that appears independent of the charging status of arginyl-tRNAs. *J. Biol. Chem.*, **274**, 37565–37574.
18. Dong,H. and Kurland,C.G. (1995) Ribosome mutants with altered accuracy translate with reduced processivity. *J. Mol. Biol.*, **248**, 551–561.
19. Kopeina,G.S., Afonina,Z.A., Gromova,K.V., Shirokov,V.A., Vasiliev,V.D. and Spirin,A.S. (2008) Step-wise formation of eukaryotic double-row polyribosomes and circular translation of polysomal mRNA. *Nucleic Acids Res.*, **36**, 2476–2488.
20. Madin,K., Sawasaki,T., Kamura,N., Takai,K., Ogasawara,T., Yazaki,K., Takei,T., Miura,K. and Endo,Y. (2004) Formation of circular polyribosomes in wheat germ cell-free protein synthesis system. *FEBS Lett.*, **562**, 155–159.
21. Yoshida,T., Wakiyama,M., Yazaki,K. and Miura,K. (1997) Transmission electron and atomic force microscopic observation of polysomes on carbon-coated grids prepared by surface spreading. *J. Electron Microsc.*, **46**, 503–506.
22. Yazaki,K., Yoshida,T., Wakiyama,M. and Miura,K. (2000) Polysomes of eukaryotic cells observed by electron microscopy. *J. Electron Microsc.*, **49**, 663–668.
23. Brandt,F., Etchells,S.A., Ortiz,J.O., Elcock,A.H., Hartl,F.U. and Baumeister,W. (2009) The native 3D organization of bacterial polysomes. *Cell*, **136**, 261–271.
24. Bernabeu,C. and Lake,J.A. (1982) Packing of 70 S Ribosomes in dimers formed at low ionic strength. Images of an unusual ribosome projection. *J. Mol. Biol.*, **160**, 369–373.

25. Wells,S.E., Hillner,P.E., Vale,R.D. and Sachs,A.B. (1998) Circularization of mRNA by eukaryotic translation initiation factors. *Mol. Cell*, **2**, 135–140.
26. Honda,M., Kaneko,S., Matsushita,E., Kobayashi,K., Abell,G. and Lemon,S. (2000) Cell cycle regulation of hepatitis C virus internal ribosomal entry site-directed translation. *Gastroenterology*, **118**, 152–162.
27. Sherrill,K.W., Byrd,M.P., Van Eden,M.E. and Lloyd,R.E. (2004) BCL-2 translation is mediated via internal ribosome entry during cell stress. *J. Biol. Chem.*, **279**, 29066–29074.
28. Liebig,H.D., Ziegler,E., Yan,R., Hartmuth,K., Klump,H., Kowalski,H., Blaas,D., Sommergruber,W., Frasel,L., Lamphear,B. *et al.* (1993) Purification of two picornaviral 2A proteinases - interaction with eIF-4g and influence on in vitro translation. *Biochemistry*, **32**, 7581–7588.
29. Imataka,H., Olsen,H.S. and Sonenberg,N. (1997) A new translational regulator with homology to eukaryotic translation initiation factor 4G. *EMBO J.*, **16**, 817–825.
30. Kuyumcu-Martinez,N.M., Van Eden,M.E., Younan,P. and Lloyd,R.E. (2004) Cleavage of poly(A)-binding protein by poliovirus 3C protease inhibits host cell translation: a novel mechanism for host translation shutoff. *Mol. Cell. Biol.*, **24**, 1779–1790.
31. Svitkin,Y.V. and Sonenberg,N. (2004) An efficient system for cap- and poly(A)-dependent translation in vitro. *Methods Mol. Biol.*, **257**, 155–170.
32. Ryan,M.D., King,A.M.Q. and Thomas,G.P. (1991) Cleavage of foot-and-mouth disease virus polyprotein is mediated by residues located within a 19 amino acid sequence. *J. Gen. Virol.*, **72**, 2727–2732.
33. Byrd,M.P., Zamora,M. and Lloyd,R.E. (2005) Translation of eIF4GI proceeds from multiple mRNAs containing a novel cap-dependent IRES that is active during poliovirus infection. *J. Biol. Chem.*, **280**, 18610–18622.
34. Van Eden,M., Byrd,M., Sherrill,K. and Lloyd,R. (2004) Translation of cellular inhibitor of apoptosis protein 1 (c-IAP1) mRNA is IRES mediated and regulated during cell stress. *RNA*, **10**, 469–481.
35. Borman,A.M., Michel,Y.M. and Kean,K.M. (2000) Biochemical characterisation of cap-poly(A) synergy in rabbit reticulocyte lysates: the eIF4G-PABP interaction increases the functional affinity of eIF4E for the capped mRNA 5′-end. *Nucleic Acids Res.*, **28**, 4068–4075.
36. Michel,Y.M., Poncet,D., Piron,M., Kean,K.M. and Borman,A.M. (2000) Cap-poly(A) synergy in mammalian cell-free extracts. Investigation of the requirements for poly(A)-mediated stimulation of translation initiation. *J. Biol. Chem.*, **275**, 32268–32276.
37. Alekhina,O.M., Vassilenko,K.S. and Spirin,A.S. (2007) Translation of non-capped mRNAs in a eukaryotic cell-free system: acceleration of initiation rate in the course of polysome formation. *Nucleic Acids Res.*, **35**, 6547–6559.
38. Khaleghpour,K., Svitkin,Y.V., Craig,A.W., DeMaria,C.T., Deo,R.C., Burley,S.K. and Sonenberg,N. (2001) Translational repression by a novel partner of human poly(A) binding protein, Paip2. *Mol. Cell*, **7**, 205–216.
39. Kahvejian,A., Svitkin,Y.V., Sukarieh,R., M'Boutchou,M.N. and Sonenberg,N. (2005) Mammalian poly(A)-binding protein is a eukaryotic translation initiation factor, which acts via multiple mechanisms. *Genes Dev.*, **19**, 104–113.
40. Sachs,A.B. and Davis,R.W. (1989) The poly(A)-binding protein is required for poly(A) shortening and 60S ribosomal subunit dependent translation initiation. *Cell*, **58**, 857–867.
41. Castello,A., Alvarez,E. and Carrasco,L. (2006) Differential cleavage of eIF4GI and eIF4GII in mammalian cells. Effects on translation. *J. Biol. Chem.*, **281**, 33206–33216.
42. Gradi,A., Svitkin,Y.V., Imataka,H. and Sonenberg,N. (1998) Proteolysis of human eukaryotic translation initiation factor eIF4GII, but not eIF4GI, coincides with the shutoff of host protein synthesis after poliovirus infection. *Proc. Natl Acad. Sci. USA*, **95**, 11089–11094.
43. Ali,I.K., McKendrick,L., Morley,S.J. and Jackson,R.J. (2001) Truncated initiation factor eIF4G lacking an eIF4E binding site can support capped mRNA translation. *EMBO J.*, **20**, 4233–4242.
44. Morino,S., Imataka,H., Svitkin,Y.V., Pestova,T.V. and Sonenberg,N. (2000) Eukaryotic translation initation factor 4E (eIF4E) site and the middle one-third of eIF4GI constitute the core domain for cap-dependent translation, and the C-terminal on-third functions as modulatory region. *Mol. Cell. Biol.*, **20**, 468–477.
45. Asselbergs,F., Peters,W., van Venrooij,W. and Bloemendal,H. (1978) Diminished sensitivity of re-initiation of translation to inhibition by cap analogues in reticulocyte lysates. *Eur. J. Biochem.*, **88**, 483–488.
46. Staehelin,T., Brinton,C.C., Wettstein,F.O. and Noll,H. (1963) Structure and function of E. Coli ergosomes. *Nature*, **199**, 865–870.
47. Uchida,N., Hoshino,S., Imataka,H., Sonenberg,N. and Katada,T. (2002) A novel role of the mammalian GSPT/eRF3 associating with poly(A)-binding protein in Cap/Poly(A)-dependent translation. *J. Biol. Chem.*, **277**, 50286–50292.
48. Hoshino,S., Imai,M., Kobayashi,T., Uchida,N. and Katada,T. (1999) The eukaryotic polypeptide chain releasing factor (eRF3/GSPT) carrying the translation termination signal to the 3′-Poly(A) tail of mRNA. Direct association of erf3/GSPT with polyadenylate-binding protein. *J. Biol. Chem.*, **274**, 16677–16680.
49. Bushell,M., Wood,W., Carpenter,G., Pain,V.M., Morley,S.J. and Clemens,M.J. (2001) Disruption of the interaction of mammalian protein synthesis initiation factor 4B with the poly(A) binding protein by caspase- and viral protease-mediated cleavages. *J. Biol. Chem.*, **276**, 23922–23928.
50. Imataka,H., Gradi,A. and Sonenberg,N. (1998) A newly identified N-terminal amino acid sequence of human eIF4G binds poly(A)-binding protein and functions in poly(A)-dependent translation. *EMBO J.*, **17**, 7480–7489.
51. Craig,A.W.B., Haghighat,A., Yu,A.T.K. and Sonenberg,N. (1998) Interaction of polyadenylate-binding protein with the eIF4G homologue PAIP enhances translation. *Nature*, **392**, 520–523.
52. Bonderoff,J.M. and Lloyd,R.E. (2008) CVB translation: lessons from the polioviruses. *Curr. Top. Microbiol. Immunol.*, **323**, 123–147.
53. Zouridis,H. and Hatzimanikatis,V. (2007) A model for protein translation: polysome self-organization leads to maximum protein synthesis rates. *Biophys. J.*, **92**, 717–730.
54. Eldad,N., Yosefzon,Y. and Arava,Y. (2008) Identification and characterization of extensive intra-molecular associations between 3′-UTRs and their ORFs. *Nucleic Acids Res.*, **36**, 6728–6738.
55. Reits,E.A., Vos,J.C., Gromme,M. and Neefjes,J. (2000) The major substrates for TAP in vivo are derived from newly synthesized proteins. *Nature*, **404**, 774–778.